Noninvasive monitoring of Pirenoxine Sodium concentration in aqueous humor based on dual-wavelength iris imaging technique

Yong Zhou,[1] Ye Hu,[1] Nan Zeng,[1] Yanhong Ji,[2] Xiangsong Dai,[1] Peng Li,[1] Hui Ma,[1] and Yonghong He[1,*]

[1]*Laboratory of Optical Imaging and Sensing, Graduate School at Shenzhen, Tsinghua University, Shenzhen, 518055, China*

[2]*MOE Key laboratory of Laser Life Science & Institute of Laser Life Science, South China Normal University, Guangzhou, 510631, China*

**heyh@sz.tsinghua.edu.cn*

Abstract: We present a noninvasive method of detecting substance concentration in the aqueous humor based on dual-wavelength iris imaging technology. Two light sources, one centered within (392 nm) and the other centered outside (850 nm) of an absorption band of Pirenoxine Sodium, a common type of drugs in eye disease treatment, were used for dual-wavelength iris imaging measurement. After passing through the aqueous humor twice, the back-scattering light was detected by a charge-coupled device (CCD). The detected images were then used to calculate the concentration of Pirenoxine Sodium. In eye model experiment, a resolution of 0.6525 ppm was achieved. Meanwhile, at least 4 ppm can be distinguished in *in vivo* experiment. These results demonstrated that our method can measure Pirenoxine Sodium concentration in the aqueous humor and its potential ability to monitor other materials' concentration in the aqueous humor.

OCIS codes: (110.2970) Image detection systems; (170.1470) Blood or tissue constituent monitoring; (170.3880) Medical and biological imaging; (170.4470) Ophthalmology.

References and links

1. R. L. Stamper, "Aqueous humor: secretion and dynamics," in *Physiology of the Human Eye and Visual System*, R. E. Records, Ed. (Harper & Row, New York, 1979).
2. M. C. Mortimer, "Tthe eye's aqueous humor, from secretion to Glaucoma," *Current Topics in Membranes*, (Academic Press, San Diego, 1998).
3. Pipe & Rapley, *Ocular Anatomy and Histology* (The association of British Opticians, London, 1999).
4. E. V. Navajas, J. R. Martins, L. A. Melo, Jr., V. S. Saraiva, C. P. Dietrich, H. B. Nader, and R. Belfort, Jr., "Concentration of hyaluronic acid in primary open-angle glaucoma aqueous humor," Exp. Eye Res. **80**(6), 853–857 (2005).
5. M. T. Leite, T. S. Prata, C. Z. Kera, D. V. Miranda, S. B. de Moraes Barros, and L. A. Melo, Jr., "Ascorbic acid concentration is reduced in the secondary aqueous humour of glaucomatous patients," Clin. Experiment. Ophthalmol. **37**(4), 402–406 (2009).
6. G. G. Koliakos, A. G. Konstas, U. Schlötzer-Schrehardt, T. Bufidis, N. Georgiadis, and A. Ringvold, "Ascorbic acid concentration is reduced in the aqueous humor of patients with exfoliation syndrome," Am. J. Ophthalmol. **134**(6), 879–883 (2002).
7. S. Pohjola, "The glucose content of the aqueous humor in man," Acta Ophthalmol. (Copenh.) **88**, 11–80 (1966).
8. B. D. Cameron, J. S. Baba, and G. L. Coté, "Measurement of the glucose transport time delay between the blood and aqueous humor of the eye for the eventual development of a noninvasive glucose sensor," Diabetes Technol. Ther. **3**(2), 201–207 (2001).
9. B. D. Cameron, H. W. Gorde, B. Satheesan, and G. L. Coté, "The use of polarized laser light through the eye for noninvasive glucose monitoring," Diabetes Technol. Ther. **1**(2), 135–143 (1999).
10. B. H. Malik, and G. L. Coté, "Real-time, closed-loop dual-wavelength optical polarimetry for glucose monitoring," J. Biomed. Opt. **15**(1), 017002 (2010).
11. B. H. Malik, and G. L. Coté, "Modeling the corneal birefringence of the eye toward the development of a polarimetric glucose sensor," J. Biomed. Opt. **15**(3), 037012 (2010).
12. J. Miller, C. G. Wilson, and D. Uttamchandani, "Minimally invasive spectroscopic system for intraocular drug detection," J. Biomed. Opt. **7**(1), 27–33 (2002).

#136682 - $15.00 USD Received 15 Oct 2010; revised 8 Dec 2010; accepted 3 Jan 2011; published 5 Jan 2011

13. J. L. Lambert, C. C. Pelletier, and M. Borchert, "Glucose determination in human aqueous humor with Raman spectroscopy," J. Biomed. Opt. **10**(3), 031110 (2005).
14. C. C. Pelletier, J. L. Lambert, and M. Borchert, "Determination of glucose in human aqueous humor using Raman spectroscopy and designed-solution calibration," Appl. Spectrosc. **59**(8), 1024–1031 (2005).
15. D. Weissbrodt, R. Mueller, J. Perrin, J. Backhaus, and J. B. Jonas, "Infrared spectroscopic examination of aqueous humor," J. Ocul. Pharmacol. Ther. **23**(1), 54–56 (2007).
16. A. J. Webb, and B. D. Cameron, "Multivariate image processing technique for noninvasive glucose sensing." Proc. SPIE 757203 (2010)
17. Y. Liu, P. Hering, and M. O. Scully, "An integrated optical sensor for measuring glucose concentration," Appl. Phys. B **54**(1), 18–23 (1992).
18. E. A. Boettner, and J. R. Wolter, "Transmission of the ocular media," Invest. Ophthalmol. **1**(6), 776–783 (1962).
19. M. Pircher, E. Götzinger, R. Leitgeb, A. F. Fercher, and C. K. Hitzenberger, "Measurement and imaging of water concentration in human cornea with differential absorption optical coherence tomography," Opt. Express **11**(18), 2190–2197 (2003).
20. D. Huang, E. A. Swanson, C. P. Lin, J. S. Schuman, W. G. Stinson, W. Chang, M. R. Hee, T. Flotte, K. Gregory, C. A. Puliafito, and J. G. Fujimoto, "Optical coherence tomography," Science **254**(5035), 1178–1181 (1991).
21. T. C. Ye, and N. L. Wang, *The atlas of clinical glaucoma*, People's Medical Publishing House, Bei Jing (2007).
22. C. Boyce, A. Ross, M. Monaco, L. Hornak, and X. Li, "Multispectral iris analysis: a preliminary study," in Proc. CVPRW'06, IEEE, pp. 51–59(2006).
23. D. M. Haaland, and E. V. Thomas, "Partial least-squares methods for spectral analysis 1: relation to other quantitative calibration methods and the extraction of qualitative information," Anal. Chem. **60**(11), 1193–1202 (1988).
24. H. M. Heise, R. Marbach, G. Janatsch, and J. D. Kruse-Jarres, "Multivariate determination of glucose in whole blood by attenuated total reflection infrared spectroscopy," Anal. Chem. **61**(18), 2009–2015 (1989).
25. H. Martens, and T. Naes, *Multivariate Calibration*, Wiley, Chichester (1991).
26. T. W. King, G. L. Cote, R. McNichols, and M. J. Goetz, Jr., "Multispectral polarimetric glucose detection using a single pockels cell," Opt. Eng. **33**(8), 2746–2753 (1994).
27. G. R. Reiss, D. A. Lee, J. E. Topper, and R. F. Brubaker, "Aqueous humor flow during sleep," Invest. Ophthalmol. Vis. Sci. **25**(6), 776–778 (1984).
28. J. S. Baba, B. D. Cameron, S. Theru, and G. L. Coté, "Effect of temperature, pH, and corneal birefringence on polarimetric glucose monitoring in the eye," J. Biomed. Opt. **7**(3), 321–328 (2002).

1. Introduction

The aqueous humor is limpid watery fluid that fills the space between the cornea and the lens in the eye [1,2]. It mainly consists of water, which takes up nearly 99 percents [3], as well as amount of glucose, proteins, ascorbate, lactate, etc. In healthy eyes, these components remain at a standard level. This level, however, may become irregular for people with eye disorders [4–6]. Moreover, since aqueous humor is formed from plasma, their compositions are almost the same. Each substance concentration in aqueous humor has a stable ratio to itself in blood [7,8]. Meanwhile, drugs to treat various eye disorders are delivered to the aqueous humor. The concentration of a drug in the aqueous humor directly reflects its bioavailability. The conventional approach to measure material concentration in the anterior chamber is to extract a sample of aqueous humor which is invasive. This technique is rarely used for investigation in human because it carries a risk of endophthalmitis.

Noninvasive sensing approaches for substances in the aqueous humor have been proposed in the past several years, including spectroscopic absorption, polarization changes, Raman spectroscopy, iris imaging analysis, and infrared spectroscopy. In 1999, Cameron et al. [9] introduced a dual wavelength laser-based polarimeter to measure glucose concentration. A resolution glucose level of 12.8 mg/dL in the curette experiments with real-time closed-loop dual-wavelength optical polarimetry was reported by Malik et al. [10,11] recently. In 2002, Miller et al. [12] designed a contact lens to detect optical absorbance spectrum of drug compounds minimally invasively. The drugs' spectra in different concentration can be distinguished in ex vivo rabbit's eye experiment. In 2005, Lambert et al [13], Pelletier et al. [14] utilized Raman spectroscopy to quantify substance concentration in the aqueous humor. A root-mean-square error of 22 mg/dL was achieved in artificial aqueous humor experiment. In 2007, Weissbrodt et al. [15] examined infrared spectroscopy of human aqueous humor and pointed out that eyes with cataract, age-related macular degeneration, or diabetic macular edema can be differentiated by the method. Such researches have provided possible solutions to monitor substance concentration in the aqueous humor.

#136682 - $15.00 USD Received 15 Oct 2010; revised 8 Dec 2010; accepted 3 Jan 2011; published 5 Jan 2011

The above mentioned works were based on point detection, which refers to light beams with small spot size shining onto the sample. The uncertainty of spatial positional signals has influence on the accuracy of measurements. This influence including the speckle-induced errors can be avoided in the iris imaging technique. Moreover, such technique can be potentially used in combination with iris recognition technology, which has been widely applied in biometrics security field at present. By adding an image processing program in current iris recognition system, the iris can be identified and substance concentration in the aqueous humor can be monitored at the same time. In 2010, a multivariate image processing technique was reported by Webb et al. [16] for noninvasive glucose sensing. Based on the refractive index change of the aqueous humor induced by glucose concentration [17], they created a calibration model to predict glucose concentration by analyzing iris image.

In this paper, we report a method to detect concentration of materials with a dual-wavelength iris imaging technique. According to the absorption spectrum of the material, two light sources with wavelengths at 392 nm and at 850 nm were selected, where the absorption coefficients are relatively the same for water but significantly different for Pirenoxine Sodium in the anterior chamber. The variations of light absorbed by the aqueous humor in the two wavelengths were measured from the iris images. The material concentration can therefore be predicted by analyzing the absorbed light. Moreover, an *in vivo* experiment was carried out to prove the feasibility of our approach.

2. Principles

The structure of a typical anterior chamber is shown in Fig. 1. A light beam with intensity I_0 passes through the aqueous humor in the anterior chamber of the eye. Since the cornea and the aqueous humor are nearly optically non-scattering, the iris could be treated as a natural reflector to scatter the beam back. The intensity I of the scattered beam from the iris after propagating through the aqueous humor with a thickness of d twice can be described by Beer's law

$$I(\lambda, d) = I_0(\lambda) e^{-2(\mu_a(\lambda)+\mu_s(\lambda))d}, \tag{1}$$

where λ is the wavelength, μ_a is the absorption coefficient and μ_s is the scattering coefficient. Considering the variation of aqueous humor's depth in different anterior chamber sites and the unequal distribution of incident light I_0, the light intensity I should be expressed as follows:

$$I(\lambda, d(\lambda, r)) = I_0(\lambda)\chi(\lambda, r) e^{-2(\mu_a(\lambda)+\mu_s(\lambda))d(\lambda,r)}, \tag{2}$$

where r denotes the distance between incidence light positions on iris and pupil center, and χ (λ, r) denotes the distribution of light intensity I according to r. Taking the logarithm of Eq. (2), we obtain

$$\ln(I(\lambda, d(\lambda, r))) = \ln(I_0(\lambda)) + \ln(\chi(\lambda, r)) - 2(\mu_a(\lambda) + \mu_s(\lambda))d(\lambda, r). \tag{3}$$

#136682 - $15.00 USD Received 15 Oct 2010; revised 8 Dec 2010; accepted 3 Jan 2011; published 5 Jan 2011

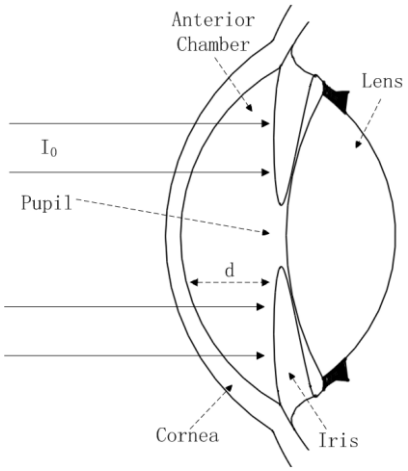

Fig. 1. The structure of anterior chamber. An incident light beam I_0 gets into the anterior chamber. After passing through the aqueous humor, the emergent light I is scattered back from the iris. Being absorbed twice by the material in the aqueous humor, the emergent light intensity I carries the information of material concentration.

By subtracting the logarithm signals acquired from the two lights, we obtain

$$\ln\left(\frac{I(\lambda_1, d(\lambda_1, r))}{I(\lambda_2, d(\lambda_2, r))}\right) = \ln\left(\frac{I_0(\lambda_1)}{I_0(\lambda_2)}\right) + \ln\left(\frac{\chi(\lambda_1, r)}{\chi(\lambda_2, r)}\right) - 2(\mu_a(\lambda_1) + \mu_s(\lambda_1))d(\lambda_1, r) + 2(\mu_a(\lambda_2) + \mu_s(\lambda_2))d(\lambda_2, r), \tag{4}$$

where subscripts 1 and 2 denote the wavelength 392 nm and 850 nm, respectively. The anterior chambers of humans and rabbits are relatively transparent between 300 and 1400 nm [18]. Since only a small amount of light scattering is present in the aqueous humor [18], the scattering of the two wavelengths is negligible compared to that of the absorption. Furthermore, as the absorption coefficient of the light with wavelength at 392 nm is far larger than that at 850 nm, the influence of the latter can be neglected. Therefore, the Eq. (4) can be reduced to

$$\ln\left(\frac{I(\lambda_1, d(\lambda_1, r))}{I(\lambda_2, d(\lambda_2, r))}\right) = \ln\left(\frac{I_0(\lambda_1)}{I_0(\lambda_2)}\right) + \ln\left(\frac{\chi(\lambda_1, r)}{\chi(\lambda_2, r)}\right) - 2\mu_a(\lambda_1)d(\lambda_1, r). \tag{5}$$

Taking the integral of Eq. (5), we obtain

$$\int_{r_1}^{r_2} \ln\left(\frac{I(\lambda_1, d(\lambda_1, r))}{I(\lambda_2, d(\lambda_2, r))}\right)dr = \int_{r_1}^{r_2} \left(\ln\left(\frac{I_0(\lambda_1)}{I_0(\lambda_2)}\right) + \ln\left(\frac{\chi(\lambda_1, r)}{\chi(\lambda_2, r)}\right)\right)dr - 2\mu_a(\lambda_1)\int_{r_1}^{r_2} d(\lambda_1, r)dr, \tag{6}$$

where integral from r_1 to r_2 corresponds to the iris area. For each sample model, r_1, r_2 were chosen according to the iris area of the images captured by the CCD. For succinct expression and analysis, we define $k = I(\lambda_1, d(\lambda_1, r))/I(\lambda_2, d(\lambda_2, r))$, which denotes the ratio of the two wavelength signals directly acquired by the CCD. And we define

$$S = -\int_{r_1}^{r_2} \ln\left(\frac{I(\lambda_1, d(\lambda_1, r))}{I(\lambda_2, d(\lambda_2, r))}\right)dr, \tag{7}$$

as special area, which denotes the logarithm ratio of two wavelengths signals reflecting from the whole iris area. As will be explained below, the special area S has a linear relationship with the material concentration c in the aqueous humor. With the absorption cross section σ_a

#136682 - $15.00 USD Received 15 Oct 2010; revised 8 Dec 2010; accepted 3 Jan 2011; published 5 Jan 2011

of the pure substance, which can be measured by traditional spectroscopy, the concentration c of the absorbing material is calculated via [19]

$$c = \mu_a(\lambda_1) \Big/ \sigma_a . \tag{8}$$

Combining Eq. (6), Eq. (7) and Eq. (8), we obtain

$$c = (S - b) \Big/ a , \tag{9}$$

where

$$b = -\int_{r_1}^{r_2} (\ln(\frac{I_0(\lambda_1)}{I_0(\lambda_2)}) + \ln(\frac{\chi(\lambda_1, r)}{\chi(\lambda_2, r)}))dr, \tag{10}$$

and

$$a = 2\sigma_a \int_{r_1}^{r_2} d(\lambda_1, r)dr. \tag{11}$$

Coefficients a and b are defined for simplification and for clear appearance of the final Eq. (9). The distribution of light intensity I according to r χ (λ, r) can be calculated by our verification experiment that is described latter in this manuscript. Thus we can obtain the exact value of b. The absorption cross section σ_a of the pure substance can be measured by traditional spectroscopy. The depth d can be measured with optical coherence tomography [20]. Therefore, coefficient a can be calculated. As a result, if we measure the special area S by our technique, the substance concentration c can be predicted.

3. Materials and experimental setup

In our experiment, Pirenoxine Sodium, which is a common kind of drug to treat cataract, was used to prove the feasibility of our approach. The Pirenoxine Sodium absorption spectrum was measured by a traditional UV spectrophotometer (DU 800, Beckman Coulter, US) and the result is shown in Fig. 2. It can be concluded from Fig. 2 that Pirenoxine Sodium has an absorption peak at 392 nm where the absorption of water is very low. In addition, both Pirenoxine Sodium and water have very low absorption at 850 nm. According to the measured absorption spectrum, two different light sources, one centered within (392 nm) and the other centered outside (850 nm) of a Pirenoxine Sodium absorption band, were utilized to image the iris.

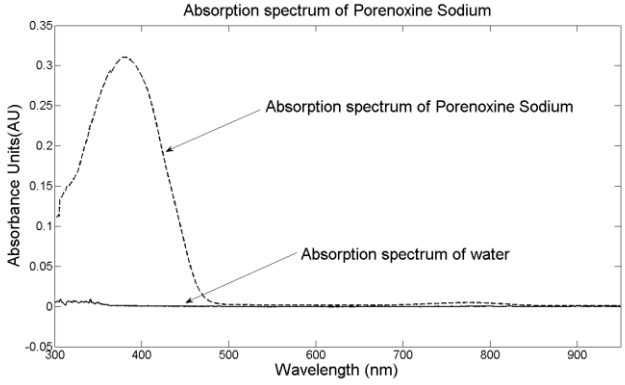

Fig. 2. The absorption spectrum of Pirenoxine Sodium measured by a commercial UV spectrophotometer. The concentration of measured Pirenoxine Sodium solution was 5.33 ppm.

#136682 - $15.00 USD Received 15 Oct 2010; revised 8 Dec 2010; accepted 3 Jan 2011; published 5 Jan 2011

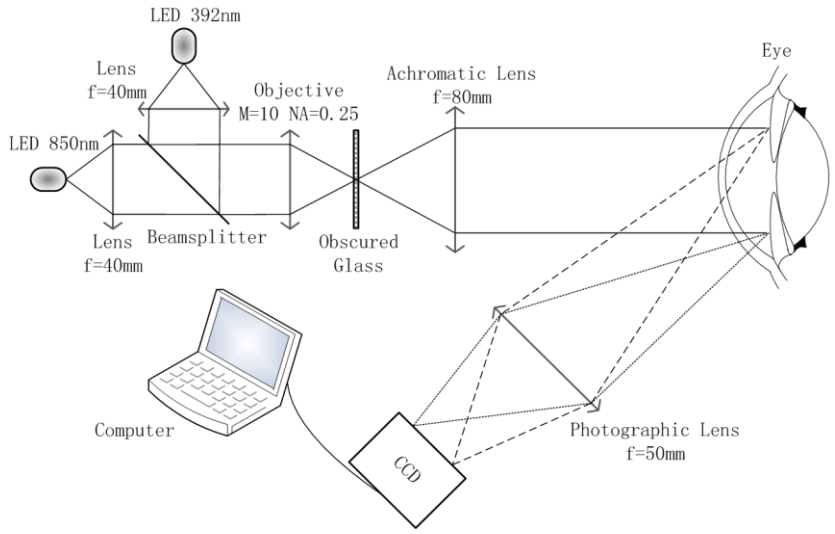

Fig. 3. The schematic used in the experiment.

Figure 3 shows the experiment setup. Two light sources were used to take the dual-wavelength iris images. The center wavelength of one Light Emitting Diode (LED) was 392 nm, the other was 850 nm. The bandwidth of 392 nm and 850 nm LED was 16 nm and 42 nm, respectively. After collimated lens, the two lights were coupled together by a beamsplitter (Edmund, Singapore). In order to use parallel light to image the whole iris, a beam expand system was introduced into this system. In addition, an obscured glass was used to eliminate the structure information of the light sources. For light source with wavelength at 392 nm and 850 nm, the power incident on the cornea was measured to be 0.43 mW/cm^2 and 0.15 mW/cm^2, respectively. The diffuse reflection light from iris was focused and detected by a CCD (Retiga EXi, Q-imaging, Canada).

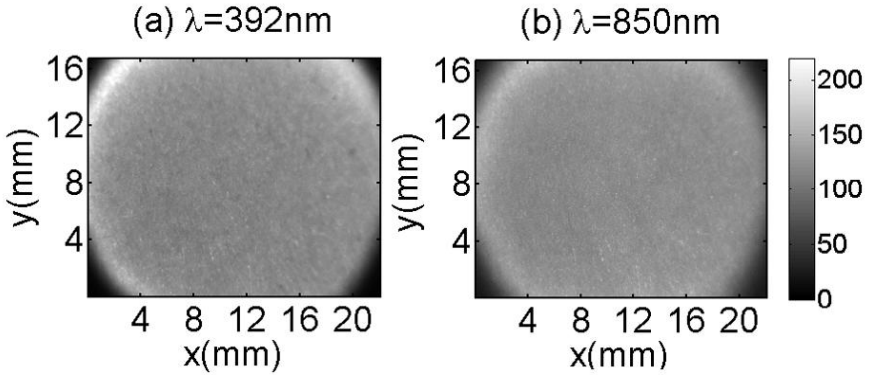

Fig. 4. The images of the paper under the illumination of both wavelengths' light.

A piece of white paper was used as the sample to verify whether the incident beam was parallel and uniform. The images of the paper under the illumination of both 392 nm and 850 nm lights are shown in Fig. 4. From Fig. 4, we can see that the two wavelengths' beam spots have nearly the same size and position. Moreover, the light intensity of each wavelength is almost the same as the radius increases. It can be concluded that the incident beams of both wavelengths were parallel and uniform.

An eye model was developed to simulate the structure of the anterior chamber. The model included a hemisphere glass shell, the liquid inside and a piece of water proof paper fastened on the shell, which represented the cornea, the aqueous humor and the iris, respectively.

#136682 - $15.00 USD Received 15 Oct 2010; revised 8 Dec 2010; accepted 3 Jan 2011; published 5 Jan 2011

Moreover, we painted the center of the paper black to represent the pupil. In the eye model experiment, we prepared a series of different Pirenoxine Sodium water solutions at the concentration of 0, 2, 4, 5, 6, 8, 10 ppm.

Due to the similarity in sizes and structures between rabbit eyes and human eyes, a New Zealand rabbit was used in the *in vivo* experiment. Pelltobarbitalum Natricum was used to anesthetize the rabbit at the beginning of the experiment. The rabbit was totally anesthetized after around ten minutes. It was then tied on the sample stage and kept still throughout the entire experiment. In this *in vivo* experiment, the Pirenoxine Sodium was injected into the rabbit anterior chamber. The volume of the rabbit anterior chamber is 250 μL [21]. The Pirenoxine Sodium solution at a concentration of 500 ppm served as the mother liquor in our experiment. We first injected 2 μL and then continued to inject 3 μL of the mother liquor into the anterior chamber. As a result, the Pirenoxine Sodium solution at concentrations of 4 ppm and 10 ppm can be successively obtained in the anterior chamber. In conclusion, three different concentrations 0, 4, 10 ppm were detected in the *in vivo* experiment.

4. Results

4.1 ZEMAX experiment

To verify the feasibility of this experiment, an analogy experiment was carried out with the ZEMAX@ software. A hemisphere model (with inner diameter of 24 mm, outer diameter of 32 mm and a refractive index of 1.5 for cornea, a refractive index of 1.34 for aqueous humor) and an anterior chamber model (with front plane curvature radius of 7.8 mm, back plane curvature radius of 6.8 mm, plane radius of 11 mm and a refractive index of 1.377 for cornea, a refractive index of 1.3374 for aqueous humor, center depth of 3 mm for aqueous humor) were set up to simulate the experiment. Experiments were completed at wavelengths of 392 nm and 850 nm in the two models, respectively. A total of 500,000,000 traced rays were used in the experiment. A ray tracing approach was employed in which the light rays were emanated in parallel from the source through the cornea and the aqueous humor. After being reflected by the iris, the light rays passed through the aqueous humor and the cornea again towards a focusing lens, and eventually were detected by an imaging detector. The simulations were completed by varying attenuate coefficients of the aqueous humor from 100 percent to 10 percent, which correspond to Pirenoxine Sodium concentration between 0 ppm to 2.36 ppm. The attenuate coefficient was defined as the ratio of the light intensity after propagating through an optical path of 25 mm to its original value. The results of the two models are shown in Fig. 5. It illustrates a strong linearity between special area S and concentration c, which demonstrates the viability to calculate the drug concentration in the aqueous humor with our approach.

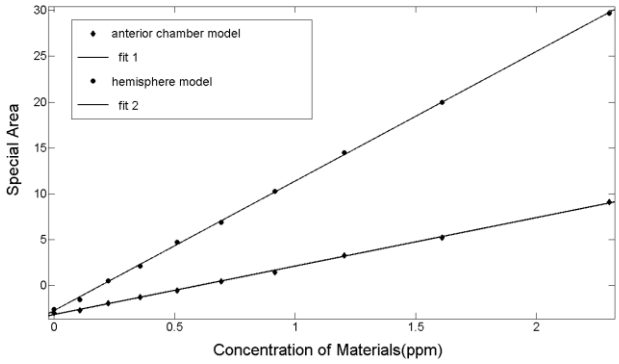

Fig. 5. The stimulation results by ZEMAX software. With different parameters set for hemisphere model and anterior chamber model, the relationship between specific area S and drug concentration c changes. Nevertheless, the linearity of S and c is strong under both models.

#136682 - $15.00 USD Received 15 Oct 2010; revised 8 Dec 2010; accepted 3 Jan 2011; published 5 Jan 2011

4.2 Model experiment

Figure 6 shows the original data recorded by the CCD. Here, as all the images satisfy the same regularity, we only show four different concentration liquids. The white dot near the center of each figure corresponds to the strong mirror reflecting signals from the cornea. Figure 6(a) and 6(b) illustrate that the light intensity distribution are uniform in the area of iris both with the two light sources if there are no absorption substances. In other pictures, the images recorded by 392 nm are darker in the middle part than their peripheral parts while there are no changes of the images recorded by 850 nm. Moreover, as the concentration increases, figures of light with wavelength at 392 nm become darker while the figures of light with wavelength at 850 nm almost stay the same.

For each image in Fig. 6, we processed the data within the dashed circle, which is only shown in Fig. 6(a) for a clearer view. The circle was divided into 500 concentric rings with the same thickness. In each ring, we used the average intensity to calculate lnk, where lnk is the logarithm of the ratio of two wavelengths light intensities recorded by the CCD. Figure 7 shows the relationship between lnk and r. There are significant differences between these curves with respect to different Pirenoxine Sodium concentrations. In Fig. 7, lnk decreases as Pirenoxine Sodium concentration increases with the same r. In addition, lnk increases as the r becomes larger. Only the pictures with r from 200 to 500 pixels in the CCD images were selected, which represent the iris' situation.

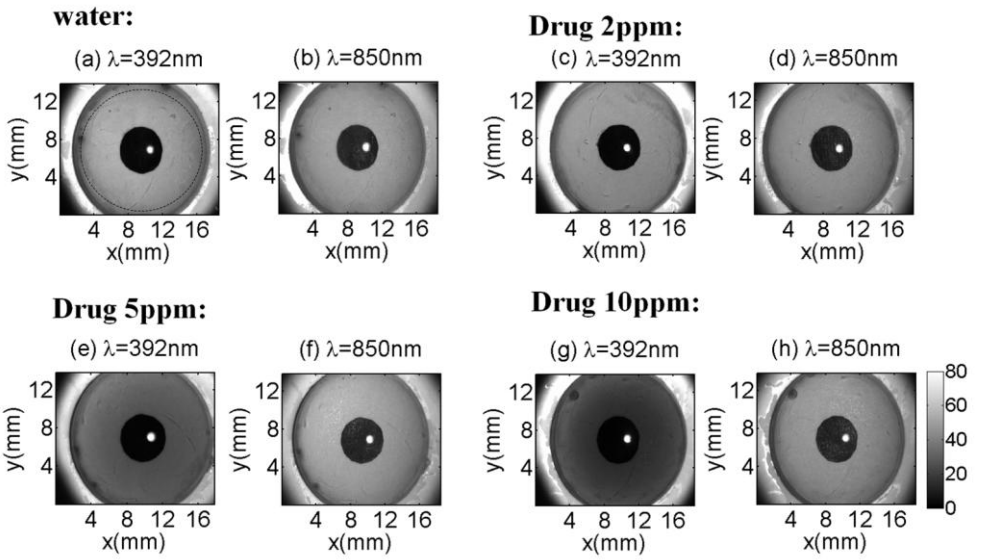

Fig. 6. Images of the anterior chamber under different Pirenoxine Sodium concentrations using two light sources with different wavelengths, one centered within the absorption band of the drug, and the other outside the absorption band. As the drug concentration increased, the images of 392nm light source got darker, while the ones of 850nm light source maintained almost unchanged. (a) We used the dashed circle area to calculate drug concentration.

#136682 - $15.00 USD Received 15 Oct 2010; revised 8 Dec 2010; accepted 3 Jan 2011; published 5 Jan 2011

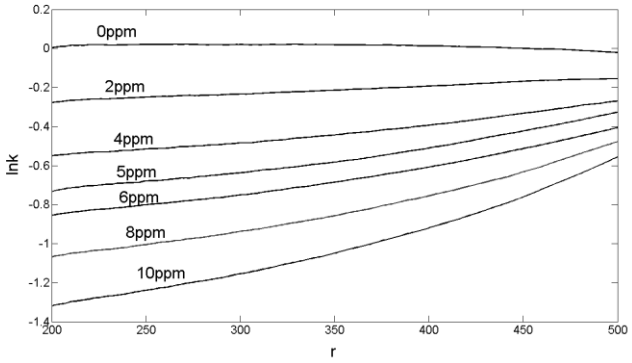

Fig. 7. Calculated lnk versus r under different Pirenoxine Sodium concentrations in the eye model experiment. As the concentration increases, the value of lnk decreases.

Figure 8 shows the computed special area S. To increase the signal-to-noise ratio of these measurements, we averaged special area S calculated from Eq. (7) over 30 measurements. The linear fitting curve in the picture can be described as

$$S = 8.324 * c - 3.024, \tag{12}$$

where the correlation coefficient is 0.9989. The system sensitivity is defined as the measured value's responsiveness to the characteristic value. The sensitivity of system can thus be expressed as

$$s = \Delta S / \Delta c, \tag{13}$$

where ΔS is the difference of S (84.02 in this experiment), and Δc is the concentration difference (10ppm in this experiment). s is therefore the slope of Eq. (12). The system sensitivity is 8.324.

The system resolution is defined as

$$\delta c = \frac{\Delta c}{\Delta S} \delta S, \tag{14}$$

where δS is the standard variation of S. When the concentration is 6 ppm, the experiment gets the maximum standard deviation of S (δS = 5.4).The resolution is calculated as 0.6525 ppm, with the maximum δS.

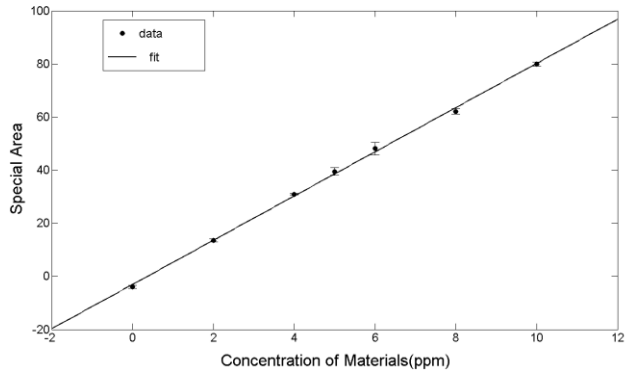

Fig. 8. The specific area S versus concentration of Pirenoxine Sodium in the eye model experiment. Data were averaged out of 30 measurements, and the error bars correspond to the standard deviation. The resolution was 0.6525 ppm.

#136682 - $15.00 USD Received 15 Oct 2010; revised 8 Dec 2010; accepted 3 Jan 2011; published 5 Jan 2011

4.3 In vivo experiment

Figure 9 shows the original pictures from the CCD in the *in vivo* experiment. As mentioned earlier, the white areas correspond to the mirror reflecting signals from cornea. If there were no absorption substances, the light intensity distributions are uniform in the area of iris in the images. When Pirenoxine Sodium concentration increases, the images obtained with the wavelength at 392 nm become darker while the ones at 850 nm remain almost unchanged.

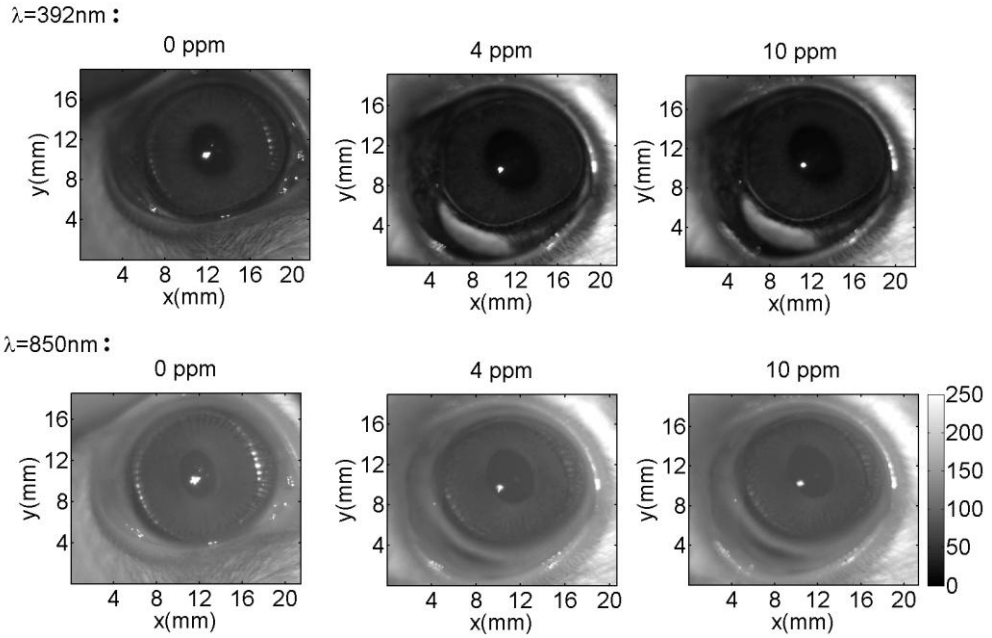

Fig. 9. Rabbit eye Images pictured by CCD with two wavelengths under different Pirenoxine Sodium concentrations.

The analysis of pictures from CCD is similar to the model experiments. Corresponding to real iris location and neglecting the pupil image, pictures with r from 140 to 300 from the CCD were selected in the *in vivo* experiment. The special area S was averaged over 30 measurements and shown in Fig. 10. The results show that the concentration c and the specific area S still meet the linearity relationship. It shows that at least 4 ppm Pirenoxine Sodium concentration can be distinguished.

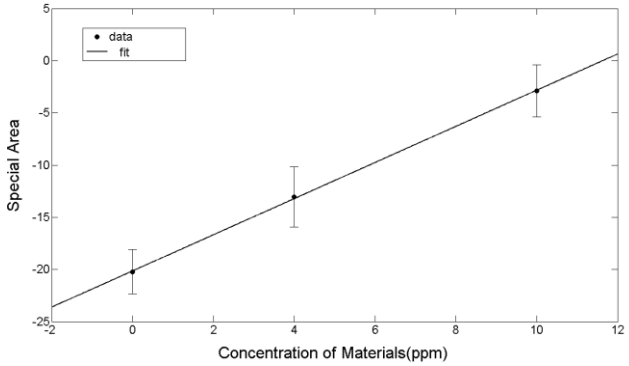

Fig. 10. The specific area S versus concentration of Pirenoxine Sodium in the *in vivo* experiment. Data are the average of 30 measurements, and the error bars correspond to the standard deviation.

#136682 - $15.00 USD Received 15 Oct 2010; revised 8 Dec 2010; accepted 3 Jan 2011; published 5 Jan 2011

5. Discussions

To illustrate the feasibility of this method, the influence resulting from the cornea should be taken into account. As explained before, we only need to analyze the change of absorption coefficient of light with wavelength at 392 nm. In the model experiment, with a hemisphere glass in place of the cornea, the absorption of the glass stays unchanged. In this situation, the influence of the cornea can be included in the coefficient b in Eq. (10). There would be no change in the experiment results. In the *in vivo* experiment, the material would penetrate into the cornea after injected into the anterior chamber. As a result, the substance concentration in the cornea would have a stable correlation with its concentration in the aqueous humor. Based on Eq. (9), the relationship between S and c remains the same, except a little change in the coefficient a:

$$a = -\sigma_a \left(\int_{r_1}^{r_2} d(\lambda_1, r) dr + \eta \int_{r_1}^{r_2} z(\lambda_1, r) dr \right), \tag{15}$$

where z (λ_1, r) denotes the depth of the cornea, and η denotes the ratio of absorption coefficient between the cornea and the aqueous humor. Therefore, taking the influence of the cornea into account would bring a change of slope in the final fit between the special area S and the concentration c without changing their linear relationship. We are still able to calculate the material concentration in the anterior chamber via the signals detected by the CCD.

In our experiment, the iris was treated as a natural reflector. The iris exhibits the same reflectance distribution at the two wavelengths of 392 nm and 850 nm that we utilized [22]. The only difference is reflectance intensity ratio at the two wavelengths for irides of different color. This influence can be included in the coefficient b in Eq. (10). Thus, considering the reflection and scattering properties of the iris for 392 nm and 850 nm would lead to no change in the experiment results.

The influences of other chemical materials in the aqueous humor are not taken into account in our experiment. We verify that our technique can monitor the Pirenoxine Sodium concentration in aqueous humor. Two possible methods can be considered in the future to reduce the influence of other materials. One is multivariate calibration techniques [23–25]; the other is to use a closed-loop system [26]. Both of them have been demonstrated to be able to compensate for the interference due to other materials potentially.

The flowing status of liquid also plays a significant role on the measurement of material concentration in the solution. The light intensities vary as the flowing status changes. Generally, the solution becomes static in two minutes after every change of the liquid based on the observation in the experiment. Since the production rate of aqueous humor is about 3.1 μL/min in the daytime [27], a dynamic equilibrium can be maintained. As a result, the change of flowing status as well as the errors from it can be ignored when the substance concentration variation is induced by its changes in blood.

In order to reduce the errors in the experiment, the temperature influence should also be considered [28]. Since the absorption coefficient changes if the temperature varies, the experiment should be carried out at the same temperature. The most critical element is that the temperature of samples should remain the same when the experiments are processed. As the aqueous humor is bounded by the cornea and iris, which are located in the eyes, the temperature stays almost constant. Compared to the external bodies, such as skin, and earlobe, which are frequently used in current material concentration detection, the changes of temperature are much smaller.

In this experiment, an obscured glass was utilized to eliminate the influence resulting from the structure of light sources and to achieve uniform light. In the future experiments, a Kohler illumination system, which can obtain the uniform light more effectively, can be utilized to improve the resolution and reduce the errors in the detection.

#136682 - $15.00 USD Received 15 Oct 2010; revised 8 Dec 2010; accepted 3 Jan 2011; published 5 Jan 2011

6. Conclusions

We developed a dual-wavelength iris imaging technology to monitor Pirenoxine Sodium concentration in the aqueous humor. We proved that the light intensities with wavelength at 392 nm declined sharply after passing through the aqueous humor with Pirenoxine Sodium while the intensities at 850 nm remained almost the same. Furthermore, as Pirenoxine Sodium concentration increased, the light intensities with wavelength at 392 nm decreased significantly whereas the intensities at 850 nm did not change much. The measurement resolution we achieved in the eye model experiment was 0.6525 ppm. Meanwhile, at least 4 ppm can be differentiated in the *in vivo* experiment using a New Zealand rabbit. These results proved the feasibility of this method to monitor Pirenoxine Sodium concentration in the aqueous humor and its potential ability to monitor other materials' concentration as well.

Acknowledgements

This research was supported by the National Science Foundation of China (NSFC), project number 61040067.

#136682 - $15.00 USD Received 15 Oct 2010; revised 8 Dec 2010; accepted 3 Jan 2011; published 5 Jan 2011